Complex anisotropy in D″ beneath the eastern Pacific from SKS–SKKS splitting discrepancies

Maureen D. Long *

Department of Terrestrial Magnetism, Carnegie Institution of Washington, 5241 Broad Branch Road, NW, Washington, DC 20015, United States

ABSTRACT

Although observations of seismic anisotropy in the lowermost mantle are abundant, the mechanism which generates anisotropy in the D″ layer is not well understood. Most observational constraints on D″ anisotropy come from the splitting of shear waves that propagate (nearly) horizontally through the lowermost mantle. However, anisotropy in the D″ layer can also give rise to discrepancies in shear wave splitting for SKS and SKKS phases for the same event-station pair, as these phases sample different regions of the lowermost mantle. Here I report observations of strongly discrepant SKS–SKKS splitting observed at broadband stations in western Mexico and California. In particular, strong SKKS splitting with fast polarization directions near ~60° and delay times up to ~3 s is observed for a group of raypaths that sample a region of the D″ layer beneath the eastern Pacific Ocean. A comparison of SKKS splitting with SKS splitting observed from the same events, as well as with SKS splitting observed at a variety of backazimuths at each station, suggests that the anomalous anisotropic structure is in the lowermost mantle. My preferred model for the unusual anisotropic geometry in this region is large shear deformation in D″ at the edge of a region where slab material impinges upon the core–mantle boundary, resulting in lattice preferred orientation of lower mantle minerals.

© 2009 Elsevier B.V. All rights reserved.

1. Introduction

The lowermost 250–300 km of the mantle, known as the D″ region, is characterized by a seismic discontinuity at its upper boundary (Sidorin et al., 1999), significant lateral heterogeneity in seismic velocity structure and, perhaps, chemical composition (Trampert et al., 2004), and regions of unusually low seismic velocities, known as ultra-low velocity zones (ULVZs) (Wen and Helmberger, 1998). Recent laboratory (Oganov and Ono, 2004; Murakami et al., 2004) and theoretical (Tsuchiya et al., 2004; Wentzcovich et al., 2006) investigations indicate that magnesium silicate perovskite, the major component of the lower mantle, likely undergoes a phase change at pressures associated with the lowermost mantle, and the presence of the post-perovskite phase has been invoked to explain some seismological properties of the D″ layer (e.g., Wookey et al., 2005b; Lay and Garnero, 2007). In addition to the considerable lateral heterogeneity, the presence of ULVZs, and the discontinuity likely associated with the post-perovskite phase change, D″ is distinguished from the overlying mantle by the presence of seismic anisotropy (e.g., Lay et al., 1998; Kendall and Silver, 1998; Moore et al., 2004).

Constraints on this anisotropy come mainly from the splitting of shear waves that propagate through D″ with nearly horizontal paths,

such as S, S_{diff}, and (at large epicentral distances) ScS (e.g., Fouch et al., 2001; Garnero et al., 2004; Wookey et al., 2005a; Rokosky et al., 2006). With the limited raypath distribution of such body-wave studies, however, it is difficult to place tight constraints on the geometry of the anisotropy. Most models for anisotropy in the D″ layer incorporate transverse isotropy with a vertical symmetry axis (VTI), but there is some evidence for more complex styles of anisotropy in several regions of D″, including tilted transverse isotropy (TTI) and/or azimuthal anisotropy (e.g., Garnero et al., 2004; Maupin et al., 2005; Wookey et al., 2005a; Thomas et al., 2007; Wookey and Kendall, 2008).

The splitting of SK(K)S phases is nearly always interpreted as being due to azimuthal anisotropy in the upper mantle beneath a seismic station; however, from a ray theoretical point of view, such phases should be also sensitive to azimuthal anisotropy in D″ (e.g., Hall et al., 2004). In particular, a comparison of shear wave splitting for SKS and SKKS arrivals for the same earthquake/station pair can provide constraints on the presence of splitting due to D″; SKS and SKKS have similar raypaths in the upper mantle, and their raypaths only diverge significantly in the lowermost mantle (Fig. 1). Observations of significant SKS–SKKS splitting discrepancies therefore likely reflect variations in azimuthal anisotropy in the deepest mantle.

Discrepancies between SKS and SKKS splitting were first documented by James and Assumpção (1996) and have been observed for a limited number of regions. Subtle differences in splitting between SKS and SKKS phases have been attributed to slightly different propagation directions through a dipping layer of upper mantle anisotropy (e.g.,

* Present address: Department of Geology and Geophysics, Yale University, PO Box 208109, New Haven, CT 06518, United States.
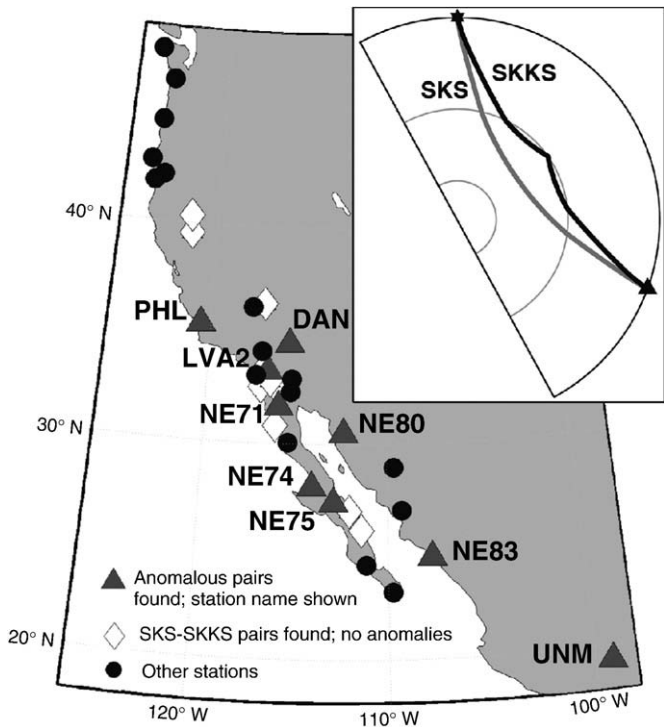 E-mail address: maureen.long@yale.edu.

Fig. 1. Station locations for all stations examined in this study. (Inset) Example of SKS and SKKS raypaths for a source (star)–receiver (triangle) distance of 115°.

Plomerová et al., 2007), but pronounced discrepancies are usually attributed to structure in the lower mantle, far away from the receiver. From a detailed regional study of SKS/SKKS splitting, Wang and Wen (2007) concluded that SK(K)S phases were affected by an anomalous region of anisotropy on the border of a very low velocity province (VLVP) in D″ beneath Africa. Global studies of SKS/SKKS differential splitting (Niu and Perez, 2004; Restivo and Helffrich, 2006) demonstrate that SKS and SKKS splitting for the same event/station pair agree within the measurement errors in approximately 95% of cases. However, in a small minority of cases, the measurements diverge significantly; Niu and Perez (2004) and Restivo and Helffrich (2006) both identified localized regions of the lower mantle that apparently contribute to discrepant SKS/SKKS splitting.

Here I present splitting measurements for SKS and SKKS waves recorded at stations in western Mexico and California. Pronounced discrepancies between SKS and SKKS splitting for the same event/station pairs are identified for a group of events located in the western Pacific that sample the lowermost mantle beneath the eastern Pacific

Ocean. SKS–SKKS pairs from earthquakes in other regions, which cover a variety of backazimuths and sample different regions of the D″ layer, do not exhibit discrepant splitting. These measurements represent an unequivocal observation of a contribution to SK(K)S splitting from anisotropy in the lower mantle, most likely in the D″ layer, and argue for a localized region of coherent azimuthal anisotropy (that is, an anisotropic geometry that results in azimuthal variations in shear velocities in a horizontal plane) in D″ beneath the eastern Pacific.

2. Data and methods

Strong, consistent splitting of SKKS phases from a group of events in the western Pacific was identified at five stations of the NARS-Baja array during routine splitting analysis to study upper mantle anisotropy (Long, M. D., Frequency-dependent shear wave splitting and heterogenous anisotropic structure beneath the Gulf of California region, in preparation). The anomalous SKKS splitting measurements exhibited fast directions (ϕ) between 45° and 65° and delay times (δt) between 1.0 and 2.7 s; the corresponding SKS phases from the same events generally exhibited little or no splitting. In order to constrain and identify the source of the anisotropy, a systematic study of SKS–SKKS differential splitting at stations in the western United States and Mexico was begun. The goal of this survey was to identify clean SKS and SKKS records with good waveform clarity and high signal-to-noise ratios for the same event-station pairs for which the shear wave splitting parameters for both phases could reliably be constrained.

Broadband waveform data for the 14 stations of the NARS-Baja array, Geoscope station UNM in central Mexico, and 16 permanent stations in California (BBR, BTC, DAC, DAN, DVT, FUR, GOR, LVA2, MIN, MONP, OLP, ORV, PHL, PLM, SMM, and WDC) were examined in this study (Fig. 1). California stations with well-constrained, simple splitting patterns that exhibited SKS splitting of less than 0.5–0.7 s (Polet and Kanamori, 2002) were preferentially selected to minimize any contribution to splitting from upper mantle anisotropy. Additionally, data from temporary Transportable Array (TA) stations in northern California, Oregon, and Washington (C03A, E03A, H02A, K01A, L02A, and M01C) were examined, but due to the limited amount of data available and the less-favorable event coverage, no usable SKS–SKKS pairs were identified at these stations. Events with magnitude ≥5.8 located in the epicentral distance range from 108° to 120° were selected for splitting analysis; this represents the distance range over which SKS and SKKS can generally be simultaneously identified for the same event-station pair. An event map is shown in Fig. 2. All records were bandpass filtered to retain energy at periods between 8–10 s and 25–50 s; for each waveform, the corner frequencies were chosen manually to optimize waveform clarity and
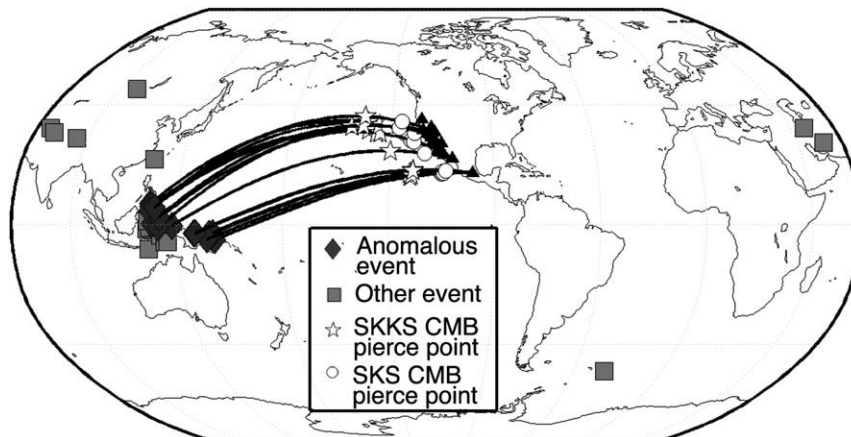

Fig. 2. Event locations for all earthquakes that yielded at least one usable SKS–SKKS splitting pair. Black lines denote great circle paths for the anomalous pairs, along with the surface projection of the receiver-side core–mantle boundary pierce point for SKKS and SKS.
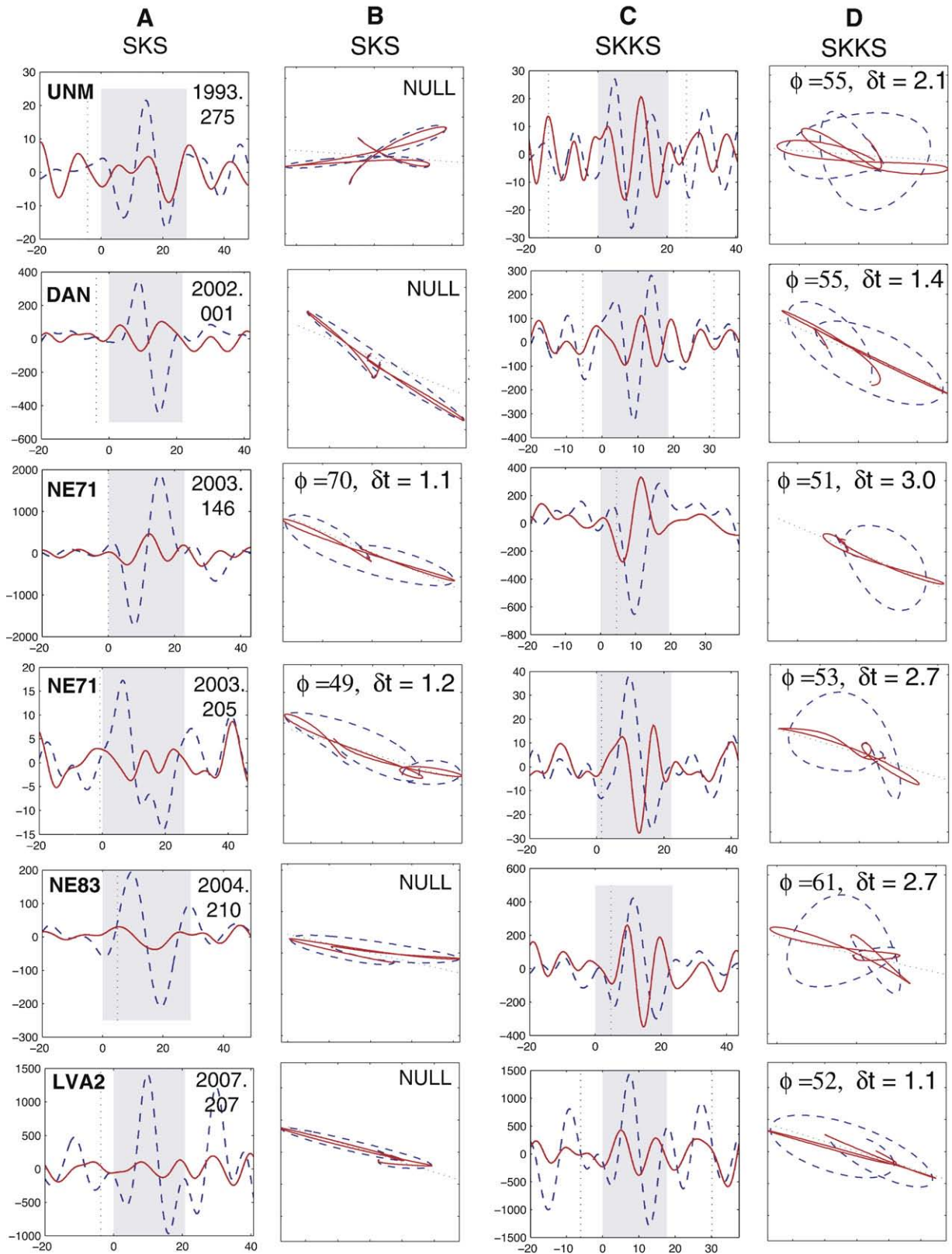
Fig. 3. Radial and transverse SKS and SKKS seismograms and particle motion diagrams for a representative set of discrepant SKS–SKKS pairs from the full data set. Six SKS–SKKS pairs are shown for which the measured splitting parameters for SKS and SKKS disagree (within the formal errors on the measurements). In column A, the radial (dashed line) and transverse (solid line) components of the SKS waveform are shown, with the station name (upper left) and event date (year and Julian day, upper right). The shaded gray region indicates the time window used in the splitting analysis. Column B shows the corresponding particle motion diagram, with the original (dashed line) particle motion shown along with the particle motion after correction with the best-fitting splitting parameters (solid line). The light dotted line indicates the backazimuth, which for SK(K)S waves corresponds to the expected initial polarization direction. The best-fitting splitting parameters (fast direction in degrees, delay time in s) are shown in the upper right corner of the particle motion diagram; null or near-null measurements are indicated by "NULL." Columns C and D show the corresponding SKKS waveforms and particle motion diagrams, respectively, for the same event-station pair shown in columns A and B.

signal-to-noise ratio. The initial polarization of each SKS and SKKS phase was measured before splitting analysis and for every arrival in the data set, the SKS and SKKS polarizations were within 10° of the

backazimuth (that is, no initial polarization anomalies were identified). This initial polarization estimate was obtained by using a covariance-based measure of the direction of maximum linearity of
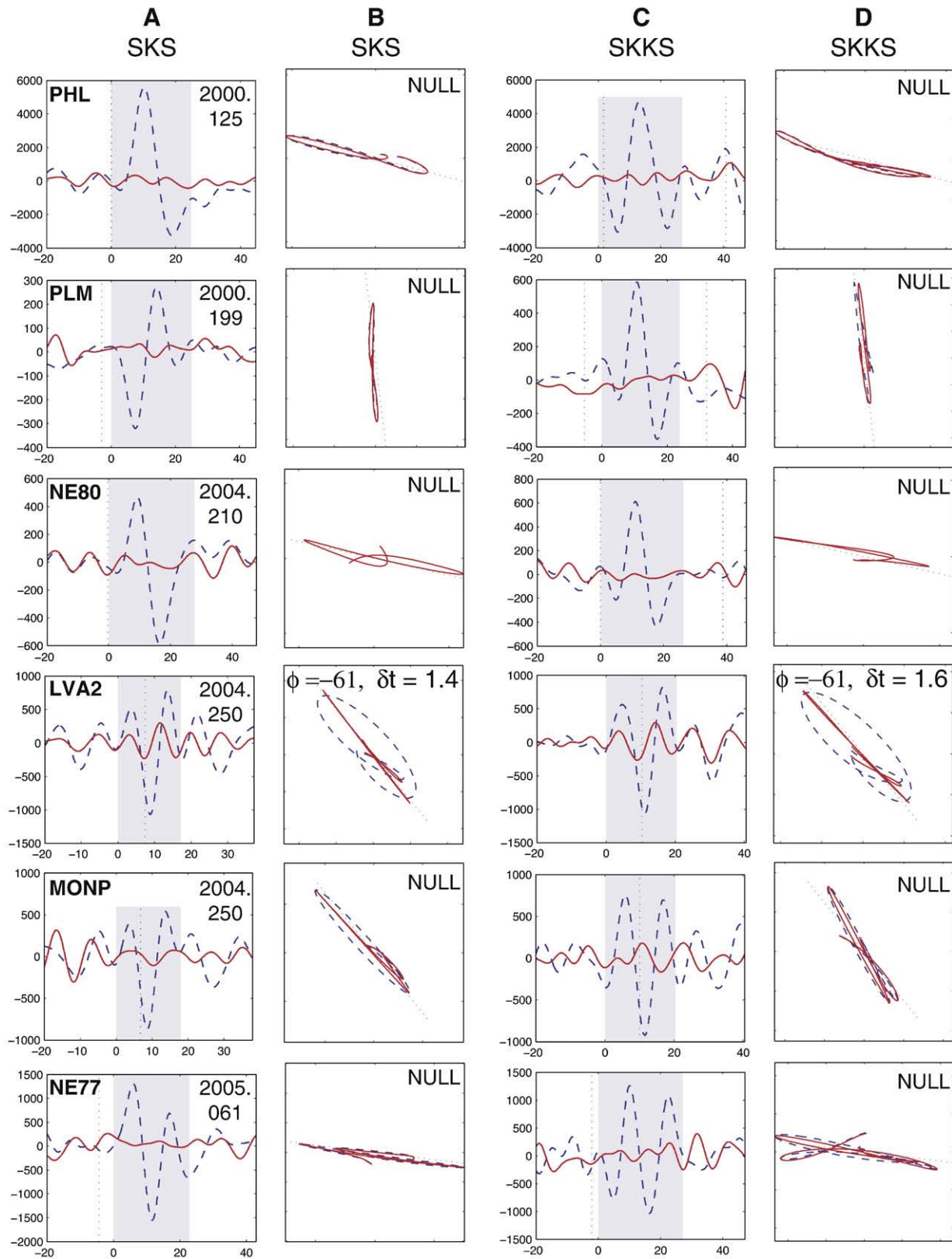

Fig. 4. Radial and transverse SKS and SKKS seismograms and particle motion diagrams for a representative set of non-discrepant SKS–SKKS pairs from the full data set. Six SKS–SKKS pairs are shown for which the measured splitting parameters for SKS and SKKS agree (within the formal errors on the measurements). The symbols and plotting conventions used are the same as in Fig. 3.

the uncorrected particle motion (e.g., Vidale, 1986); for the case where the delay time δt is much smaller than the dominant period of the shear wave, this procedure yields an accurate estimate of the initial polarization (e.g., Long and van der Hilst, 2005).

Splitting measurements were made with both the cross-correlation method (e.g., Levin et al., 1999) and the transverse component minimization method (Silver and Chan, 1991) using the SplitLab software (Wüstefeld et al., 2007). Only records where splitting parameter estimates using the two methods agreed within the 2σ formal errors were retained, since these methods can disagree for noisy data or complex or near-null splitting (Long and van der Hilst, 2005; Wüstefeld and Bokelmann, 2007). The use of multiple measurement methods helps to ensure that only records for which splitting parameters could be reliably estimated are retained (e.g., Levin et al., 2004; Long and van der Hilst, 2005). Records characterized by high signal-to-noise ratio, good waveform clarity, and linear initial particle motion (that is, little or no energy on the transverse component) were classified as nulls. Properly defined, null measurements do not include noisy records with poor waveform clarity and such records were not characterized as null measurements in this study. For simplicity I report the results using the Silver & Chan method in the paper, but all of the measurements reported here yielded consistent splitting parameters using both measurement methods. The complete set of splitting parameter measurements was then mined to identify high-quality measurements for both SKS and SKKS phases using the same event-station pair. This procedure yielded a total of 52 SKS–SKKS pairs at 19 different stations for which splitting parameters for both phases were well constrained; station and event information for all pairs are shown in Supplementary Table S1. Representative examples of SKS and SKKS waveforms and particle motion diagrams are shown in Figs. 3 and 4. Fig. 3 shows SKS–SKKS pairs that exhibit splitting discrepancies; Fig. 4 shows pairs that do not.

3. Results

An example of splitting analysis for an SKS–SKKS pair is shown in Fig. 5 and splitting parameters for all SKS–SKKS pairs can be found in Supplementary Table S1. 52 well-resolved SKS–SKKS pairs were identified in the data set. Of these, 15 pairs can be labeled "anomalous". Significant discrepancies between SKS and SKKS splitting were observed for 14 of the anomalous SKS–SKKS pairs. An additional anomalous pair was identified at station PHL for which both the SKS and SKKS waves exhibited strong, similar splitting (SKS: $\phi = 62° \pm 8°$, $\delta t = 2.1$ s ± 0.3 s; SKKS: $\phi = 42° \pm 12°$, $\delta t = 2.1$ s ± 0.5 s); however, all other SKS and SKKS measurements at PHL from a variety of backazimuths were null or near-null. All of the anomalous SKS–SKKS pairs come from a localized group of events in the western Pacific (Fig. 2), with backazimuths between ~270° and 290°. No splitting discrepancies were observed for SKS–SKKS phases coming in from other backazimuths. Of the 15 anomalous SKS–SKKS pairs, 12 involve recordings of null or near-null splitting for SKS phases, but significant splitting of SKKS phases. Two of the 15 anomalous pairs, both measured at station NE71, exhibit similar fast directions but a moderate degree of SKS splitting ($\delta t \sim 1.0$ s) and significantly larger SKKS splitting ($\delta t \sim 2.5$–3.0 s). The anomalous pairs seem to exhibit geographical trends: of the 20 SKS–SKKS pairs measured at Mexican stations, 12 (60%) were anomalous; at stations further to the north in California, only 3 out of 32 (8%) exhibited anomalous splitting. This regional difference is somewhat dominated by the southernmost Mexican station (UNM), where 6 out of 7 pairs exhibited SKS–SKKS splitting discrepancies.

4. Source and geometry of the anomalous splitting

SKKS splitting parameters for the 15 anomalous SKS–SKKS pairs measured at 9 different stations are remarkably consistent: fast directions range from 42° to 65°, with most between 50° and 55°, while delay times range from ~1.0 s to ~3.1 s. The larger δt values are at the high end of the range of delay times observed globally for SK(K)S-type phases (e.g., Fouch and Rondenay, 2006). The narrow range of fast polarization directions strongly suggests that this group of SKKS arrivals is sampling a coherent region of anisotropy somewhere in the mantle on the receiver side that is not affecting the corresponding SKS phases. Discrepancies in splitting between SKS and SKKS could be explained
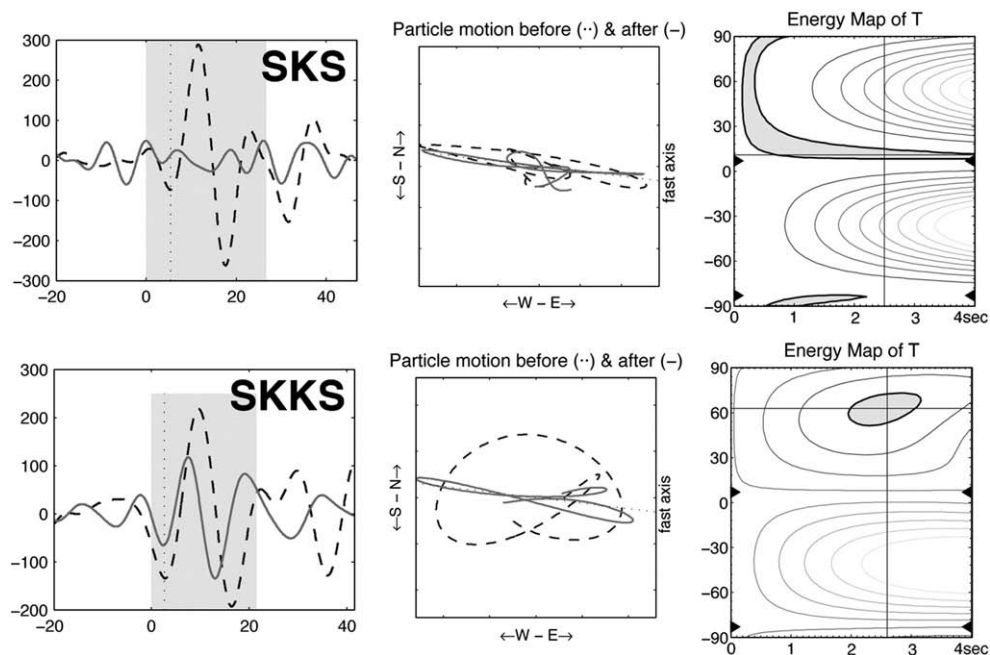

Fig. 5. An example of an anomalous SKS–SKKS splitting measurement made using the transverse component minimization method at station UNM for an event (Mw = 6.7, backazimuth = 277°, depth = 11 km, $\Delta = 118°$) in the New Britain subduction zone. Columns show the radial (dashed) and transverse (solid) components of the phase (left panels), the initial (dashed) and corrected (solid) particle motion (center panels), and the energy map of the transverse component for all possible (ϕ, δt) pairs (right panels). (Top row): The SKS phase exhibits little transverse energy, linear particle motion, and null or near-null splitting. (Bottom row): The SKKS phase exhibits strong transverse energy, elliptical particle motion, and clear evidence of splitting: well-constrained splitting parameters of $\phi = 63°$, $\delta t = 2.6$ s are obtained.
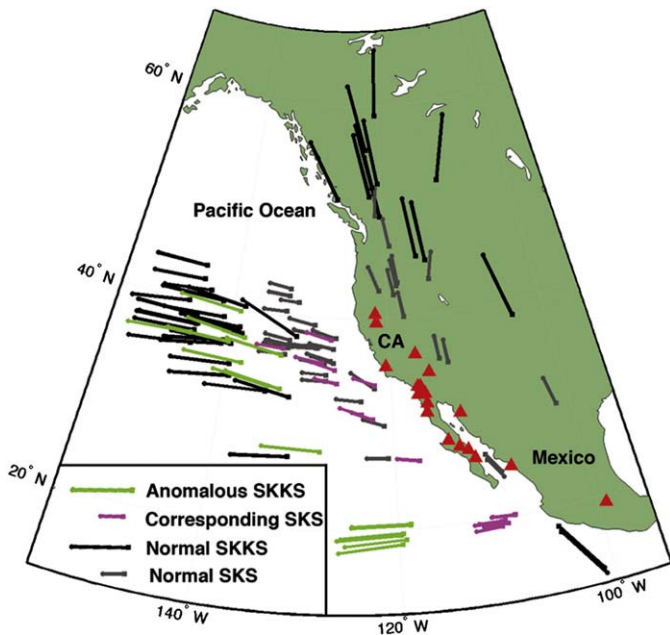
Fig. 6. A map view of D″ paths for all SKS–SKKS pairs in the data set, with anomalous pairs highlighted in color.

by a single region of anisotropy, perhaps in the upper mantle, if the initial polarizations were different, as the effect of anisotropy depends on the incoming polarization. However, since the initial polarizations for the SK(K)S waves under study were measured and found to be controlled by the P-to-S conversion at the core–mantle boundary (CMB), this scenario can be discarded.

Could the observed discrepancies be due to anisotropic structure in the upper mantle, perhaps due to a dipping symmetry axis or multiple layers of anisotropy? This scenario is extremely unlikely, for several reasons. Because no incoming polarization anomalies were detected in the SK(K)S waves under study, splitting discrepancies due to upper mantle anisotropy would have to arise due to the difference in propagation directions between the two types of waves. In the upper mantle, however, these differences in propagation direction are extremely slight (less than ~5°) and unreasonably high intrinsic anisotropy would be needed to generate splitting discrepancies of up to 3 s for such small differences in propagation direction. A second line of argument against an upper mantle source for the discrepancies comes from previous work on the magnitude of splitting due to upper mantle anisotropy (inferred from SKS splitting measured for a variety of different backazimuths). SKS splitting for a subset of the NARS-Baja stations was previously studied by Obrebski et al. (2006) and by Long (in prep.), who looked at the frequency dependence of SKS splitting. Both of these studies found that SKS delay times, presumably due to upper mantle anisotropy, are relatively small; for the stations at which SKS–SKKS splitting discrepancies were identified, Obrebski et al. (2006) generally found delay times of less than ~1 s, while Long (in prep.) found that stations NE75, NE80, and NE83 all exhibited null SKS splitting at a variety of backazimuths at periods greater than 8–10 s. California stations with small SKS delay times (Polet and Kanamori, 2002) were also preferentially selected to minimize the contribution from upper mantle anisotropy. These previous studies and the large number of well-resolved null SKS measurements from a variety of backazimuths found in this study (Supplementary Table S1) all suggest that for most stations examined here and for the low frequency part of the waveforms (periods greater than 8–10 s) there is usually little or no contribution to SK(K)S phases from upper mantle anisotropy.

The region most likely to cause the observed discrepancies, therefore, is the deepest mantle, as this is the least similar portion

of the SKS/SKKS path (inset, Fig. 1). A Fresnel zone argument (Alsina and Snieder, 1995) would indicate that for SK(K)S phases with characteristic periods of ~10 s, the regions of sensitivity should overlap significantly in the transition zone and in the upper portions of the lower mantle. (As discussed in Section 5, however, the small-scale lateral heterogeneity in anisotropic structure required by the data set somewhat weakens any argument based on finite-frequency wave propagation effects, such as the Fresnel zone argument invoked here.) Because there is considerable seismological evidence for anisotropy in the D″ layer, and because there is laboratory and seismological evidence that the bulk of the lower mantle is seismically isotropic (Meade et al., 1995), my preferred interpretation of the anomalous SKKS splitting described here is that it is due to azimuthal anisotropy (that is, anisotropic structure with azimuthal velocity variations in the horizontal plane) in D″ (see also Restivo and Helffrich, 2006; Wang and Wen, 2007). However, a contribution to the observed splitting from elsewhere in the lower mantle on the receiver side cannot be completely ruled out.

Proceeding with this line of reasoning, the D″ paths for SKS and SKKS for all pairs in the data set are plotted in Fig. 6, with the anomalous pairs highlighted. The anomalous SKKS splitting appears to delineate a region beneath the eastern Pacific that roughly parallels the west coast of North America. The unusual SKKS splitting behavior is not observed uniformly in this region; similar small-scale variations in D″ splitting have also been observed for horizontally propagating phases (e.g., Garnero et al., 2004). In contrast to the region of anomalous SKKS splitting beneath the eastern Pacific, shear arrivals that sample the D″ region beneath North America show no indication of a contribution from D″ anisotropy (Fig. 6). These results are broadly consistent with findings by Niu and Perez (2004) and Restivo and Helffrich (2006) that identified SKS–SKKS discrepancies in the lower mantle to the west of the North American coast.

The inferred orientation and strength of D″-associated splitting is shown in Fig. 7, where SKKS splitting parameters for the 15 anomalous pairs are plotted at the midpoint of the SKKS path through D″, along with the anomalous SKS splitting observed at station PHL. For the two pairs measured at station NE71, SKKS splitting has been corrected to account for the non-null SKS splitting (inferred to represent upper mantle anisotropy) by subtracting the SKS delay time from that of SKKS (given the similar fast directions, this simple subtraction is valid). In the southern part of the region of inferred anomalous anisotropy, SKKS phases exhibit the largest delay times (up to 3.1 s) but also exhibit the largest scatter in fast directions. Further to the
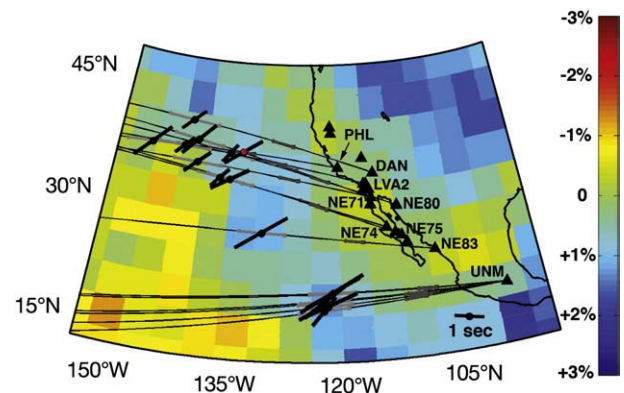

Fig. 7. Shear wave splitting parameters for anomalous SKKS phases are plotted at the midpoint of their D″ paths; the corresponding SKS paths are also shown. The anomalous SKS measurement at station PHL is also plotted at the midpoint of the SKS path and is marked with a red dot. The colors indicate isotropic S wavespeeds at the base of the mantle from the model of Houser et al. (2008) as a % deviation from the reference model. The splitting measurements are plotted in the geographical reference frame associated with the receiver; as shown in Fig. 8, however, the geometry of the raypath and fast splitting direction should be considered in a 3-D framework.
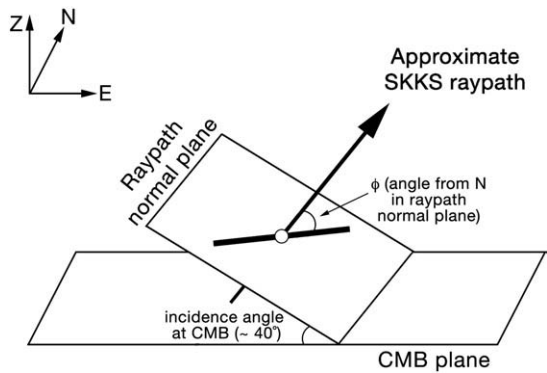
Fig. 8. A sketch of the raypath geometry above the CMB and the geometry of the fast splitting direction in the D″ layer inferred from the anomalous SKKS splitting measurements presented in this study. For simplicity, the example shown is for a backazimuth of 270° − for anomalous SKS–SKKS pairs in the data set, backazimuths range from ~271° to 294°. The thick black line with the white circle at its center denotes the fast splitting vector, which is contained in the plane normal to the raypath.

north, the measured fast directions are remarkably uniform (~50°–60°) but there is more variation in delay times (~1.0–2.1 s). If the anisotropy is confined to the D″ layer, and a path length through D″ of ~350–400 km is assumed, an intrinsic anisotropy of about 1–3% is needed to generate the observed splitting.

Because the raypaths of the anomalously split SKKS phases deviate significantly from the vertical in the D″ layer (Fig. 1), the SKKS splitting measurements plotted in Fig. 7 (and the inferred geometry of the anisotropy) must be considered in a 3-D reference frame in order to be properly interpreted. A sketch of the raypath and fast splitting direction geometry relative to the CMB is shown in Fig. 8. The fast splitting vector is contained in the plane perpendicular to the ray propagation direction, which for the SKKS paths considered here (backazimuths between 270° and 290°) dips roughly to the east. This fast splitting direction is not consistent with the simple VTI geometry that is often inferred in studies of D″ anisotropy and instead requires a more complex geometry that includes azimuthal variations in the horizontal plane (that is, azimuthal anisotropy). Further interpretation of the fast splitting vector depends on the elastic properties of the anisotropic medium, as discussed below.

5. Discussion

The anomalous SKKS splitting appears to delineate a region of fairly uniform azimuthal anisotropy in the D″ layer beneath the eastern Pacific; this region coincides geographically with a gradient in isotropic S wavespeed structure at the base of the mantle (e.g., Houser et al., 2008), as shown in Fig. 7. In general, the corresponding SKS phases from the anomalous SKS–SKKS pairs do not exhibit splitting that can be attributed to D″ anisotropy, with one exception: for the anomalous pair measured at station PHL, both the SKS and SKKS phases are anomalously split. These observations could be explained either by a region of anomalous D″ anisotropy sampled by SKKS phases but not by corresponding SKS phases, or by a homogenous anisotropic geometry that would produce significant splitting at the propagation directions associated with SKKS but not with SKS. Because the anomalous SKS phase observed at station PHL also samples the region of inferred anisotropy (Fig. 7), the former scenario seems more likely. I therefore infer that the anomalous observation of both SKS and SKKS splitting for a single event at station PHL is due to the raypath geometry: the SKS phase in question samples the D″ layer further to the west than the discrepant SKS–SKKS pairs in the data set (Fig. 7) and unlike many other SKS phases in the data set, it also samples the inferred region of anomalous D″ anisotropy.

One possible explanation for a localized region of complex anisotropic structure beneath the eastern Pacific is that it is associated with the impingement of downgoing slab materials upon the CMB.

There is ample evidence from global tomographic models for a high-velocity anomaly beneath North America that may be associated with a downgoing slab (e.g., Houser et al., 2008), and the boundary of this anomaly in the lowermost mantle coincides geographically with the inferred region of anomalous anisotropy, as shown in Fig. 7. Numerical models of a downgoing slab in the lowermost mantle by McNamara et al. (2002) predict large-scale regions of significant shear deformation near the CMB for a downgoing slab model. In these models, a downgoing slab results in a broad region of high-stress deformation in the dislocation creep regime; at the edges of this region, deformation is particularly strong and there are sharp gradients in the deformation geometry. One plausible model for the observed azimuthal anisotropy, therefore, is that it is associated with strong deformation at the edge of a region of D″ affected by the long-lived subduction of the Farallon plate beneath North America (Lithgow-Bertelloni and Richards, 1998). The observed SKKS fast directions (45°–65°) are roughly perpendicular to the edge of the continental margin; this suggests that the geometry of the anisotropy may be controlled by the geometry of the Farallon subduction zone.

The region of particularly strong deformation with sharp gradients in deformation geometry suggested by the McNamara et al. (2002) model could result in azimuthal anisotropy if fabric is generated by either the shape preferred orientation (SPO) of elastically distinct material or by the lattice preferred orientation (LPO) of lowermost mantle minerals that have been deformed by dislocation creep (e.g., Kendall and Silver, 1998; Karato, 1998; Wenk et al., 2006). The effect of D″ anisotropy on SK(K)S phases was studied in detail by Hall et al. (2004) and they found that the only SPO-type models that are efficient at generating significant SK(K)S splitting are those that include vertically oriented sheets of melt. While this mechanism cannot be ruled out for this data set, it seems unlikely that there is significant partial melt here, as this region of D″ is not associated with ultra-low velocity zones (ULVZs) that may indicate the presence of partial melt (e.g., Kendall and Silver, 1998). Further studies on the possible presence of partial melt in this region should provide additional evidence for or against an SPO-type model.

An LPO mechanism could generate azimuthal anisotropy in D″ (e.g., Yamakazi and Karato, 2007), with a possible contribution from perovskite/post-perovskite, (Mg,Fe)O, or both. Initial studies of LPO development in post-perovskite (Yamazaki et al., 2006; Merkel et al., 2007) have had some difficulty reconciling laboratory results with seismological observations, due in part to uncertainty in the single-crystal elastic constants at D″ conditions (for an overview, see Wookey and Kendall, 2007). (Mg,Fe)O would likely make a significant contribution to LPO-type anisotropy even though it represents ~25% of the lower mantle by volume, as MgO has an intrinsic shear wave anisotropy of nearly 50% at lowermost mantle pressures (Karki et al., 1997). Even in a (post)-perovskite–(Mg,Fe)O mixture, (Mg,Fe)O may dominate the anisotropic signature (e.g., Yamazaki and Karato, 2002, 2007; Yoshino and Yamazaki, 2007), particularly since deformation may be partitioned into (Mg,Fe)O as the weaker phase.

Long et al. (2006) predicted shear wave splitting in D″ from experimentally determined (Mg,Fe)O LPO patterns and found that the amount of splitting is strongly dependent on both the propagation direction of the phase of interest and on the geometry of deformation at the CMB. At large epicentral distances ($\Delta = 108°$–$120°$), the propagation directions of SK(K)S phases in D″ deviate significantly from the vertical and significant splitting of SK(K)S waves is generally consistent with the LPO patterns found by Long et al. (2006). A contribution to SK(K)S splitting from (Mg,Fe)O is even more likely if the shear plane is tilted even slightly (~10°–15°) from the horizontal. The observed delay times could be explained by the LPO of lowermost mantle phases, dominated by ferropericlase; Long et al. (2006) predicted maximum shear wave anisotropy of up to 11% in a pure (Mg,Fe)O assemblage, so 1–3% anisotropy for an (Mg,Fe)O–(post)-perovskite lower mantle assemblage would be reasonable. Despite the

uncertainties in extrapolating experimental data to lowermost mantle conditions, the available constraints suggest that LPO of lowermost mantle minerals could produce the azimuthal anisotropy inferred here. A model that invokes strong deformation resulting in LPO of a (post-)perovskite–ferropericlase aggregate at the edge of a downgoing slab region therefore seems to be a plausible explanation for the SKS–SKKS discrepancies documented in western North America.

The sharp gradients in deformation geometry suggested by models such as that of McNamara et al. (2002) might also account for the extreme small-scale heterogeneity that must be present to account for the spatial distribution of anomalous and non-anomalous SKS and SKKS paths. As demonstrated in Fig. 6, there are several examples of "normal" SKS–SKKS pairs that have very similar raypaths (and therefore sample the D″ region in a similar way) to adjacent anomalous SKS–SKKS pairs. From a ray theoretical point of view, dramatic small-scale heterogeneity in anisotropic structure is required to explain these observations; such lateral heterogeneity has also been inferred in other studies of complex anisotropic structure in D″ (e.g., Garnero et al., 2004). If finite-frequency effects are taken into account, the variations in splitting observations over such small length scales become more difficult to explain, as the sensitivity to anisotropic structure would be spread out over a finite region surrounding the ray theoretical path. The observation of small-scale lateral heterogeneity in splitting behavior (and presumably in anisotropic structure) is robust, however, both in the data set presented here and in other data sets (e.g., Fouch et al., 2001; Garnero et al., 2004; Rokosky et al., 2006; Wang and Wen, 2007). Identifying geodynamical models that can explain such small-scale heterogeneity, particularly when finite-frequency wave propagation effects are taken into account, remains a significant challenge for studies of D″ anisotropy.

6. Conclusions

The data set presented here represents a clear, unequivocal observation of strongly discrepant SKS/SKKS splitting observed at 9 different stations in western North America. The differential splitting of SKKS and SKS phases from the same earthquake-station pair provides a useful diagnostic of seismic anisotropy – more specifically, of likely lateral gradients in anisotropic structure – in the lowermost mantle. Because SKKS-SKS splitting discrepancies are the exception, and not the rule, their observation points to locally unusual anisotropic structure in D″. My preferred model to explain this observation is that shear deformation associated with the impingement of the Farallon slab upon the CMB induces the LPO of lowermost mantle minerals to produce a region of anomalous D″ anisotropy that is sampled by SKKS phases recorded in western North America. A model that invokes a downgoing slab and an associated transition in deformation geometry for this region is plausible, given the likely presence of slab material near the CMB due to long-lived Farallon subduction (Lithgow-Bertelloni and Richards, 1998) and the region's proximity to sharp lateral gradients in seismic velocities (e.g., Houser et al., 2008) and in radial anisotropy (Panning and Romanowicz, 2006). It is noteworthy that one of the few other studies to identify a systematic regional contribution of lowermost mantle anisotropy to SK(K)S splitting (Wang and Wen, 2007) also found unusual anisotropy on the edge of a large-scale velocity anomaly in the lowermost mantle; this shared proximity to a sharp lateral gradient in velocity structure (and, perhaps, a corresponding transition in deformation geometry) is suggestive. Future studies of SKKS/SKS splitting discrepancies, particularly for regions of D″ associated with downgoing slabs and in combination with constraints from other types of data, such differential ScS/S splitting, should help to constrain models for anisotropy and contribute to our understanding of the dynamics of the D″ region.

The observations presented here also sound a note of caution for the interpretation of SK(K)S splitting in terms of upper mantle anisotropy, as they demonstrate that azimuthal anisotropy in the lower mantle can make a significant contribution to the splitting of core-refracted phases. In order to rule out contributions from the lower mantle, SKKS and SKS phases from a range of backazimuths should be routinely examined for splitting discrepancies in studies of upper mantle anisotropy, particularly when regions of D″ that may be associated with non-horizontal deformation are being sampled. The combination of SK(K)S splitting measurements with measurements of direct teleseismic S phases from deep events, which do not sample the D″ region at epicentral distances between 40° and 80°, can also help to evaluate and account for any contribution to SK(K)S splitting from the lowermost mantle (e.g., Long and van der Hilst, 2005).

Appendix A. Supplementary data

Supplementary data associated with this article can be found, in the online version, at doi:10.1016/j.epsl.2009.04.019.

References

Alsina, D., Snieder, R., 1995. Small-scale sublithospheric continental mantle deformation: constraints from SKS splitting observations. Geophys. J. Int. 123, 431–448.
Fouch, M.J., Fischer, M.K., Wysession, M.E., 2001. Lowermost mantle anisotropy beneath the Pacific: imaging the source of the Hawaiian plume. Earth Planet. Sci. Lett. 190, 167–180.
Fouch, M.J., Rondenay, S., 2006. Seismic anisotropy beneath stable continental interiors. Phys. Earth Planet. Inter. 158, 292–320.
Garnero, E.J., Maupin, V., Lay, T., Fouch, M.J., 2004. Variable azimuthal anisotropy in Earth's lowermost mantle. Science 306, 259–261.
Hall, S.A., Kendall, J.-M., van der Baan, M., 2004. Some comments on the effects of lower-mantle anisotropy on SKS and SKKS phases. Phys. Earth Planet. Inter. 146, 469–481.
Houser, C., Masters, G., Shearer, P., Laske, G., 2008. Shear and compressional velocity models of the mantle from cluster analysis of long-period waveforms. Geophys. J. Int. 174, 195–212.
James, D.E., Assumpçao, M., 1996. Tectonic implications of S-wave anisotropy beneath SE Brazil. Geophys. J. Int. 126, 1–10.
Karato, S.-i., 1998. Some remarks on the origin of seismic anisotropy in the D″ layer. Earth Planets Space 50, 1019–1028.
Karki, B.B., Stixrude, L., Clark, S.J., Warren, M.C., Ackland, G.J., Crain, J., 1997. Structure and elasticity of MgO at high pressure. Am. Mineral. 82, 51–60.
Kendall, J.-M., Silver, P.G., 1998. Investigating causes of D″ anisotropy. In: Gurnis, M., et al. (Ed.), The Core–Mantle Boundary Region. Geodyn. Ser., vol. 28. AGU, Washington, DC, pp. 97–118.
Lay, T., Garnero, E.J., 2007. Reconciling the post-perovskite phase with seismological observations of lowermost mantle structure. In: Hirose, K., et al. (Ed.), Post-perovskite: The Last Mantle Phase Transition. Geophys. Monogr., vol. 174. AGU, Washington, DC, pp. 129–153.
Lay, T., Williams, Q., Garnero, E.J., Kellogg, L., Wysession, M.E., 1998. Seismic wave anisotropy in the D″ region and its implications. In: Gurnis, M., et al. (Ed.), The Core–Mantle Boundary Region. Geodyn. Ser., vol. 28. AGU, Washington, DC, pp. 299–318.
Levin, V., Droznin, D., Park, J., Gordeev, E., 2004. Detailed mapping of seismic anisotropy with local shear waves in southeastern Kamchatka. Geophys. J. Int. 158, 1009–1023.
Levin, V., Menke, W., Park, J., 1999. Shear wave splitting in the Appalachians and the Urals: a case for multilayered anisotropy. J. Geophys. Res. 104, 17975–17993.
Lithgow-Bertelloni, C., Richards, M.A., 1998. The dynamics of Cenozoic and Mesozoic plate motions. Rev. Geophys. 36, 27–78.
Long, M.D., van der Hilst, R.D., 2005. Estimating shear-wave splitting parameters from broadband recordings in Japan: a comparison of three methods. Bull. Seism. Soc. Am. 95, 1346–1358.
Long, M.D., Xiao, X., Jiang, Z., Evans, B., Karato, S.-i., 2006. Lattice preferred orientation in deformed polycrystalline (Mg,Fe)O and implications for seismic anisotropy in D″. Phys. Earth Planet. Inter. 156, 75–88.

Maupin, V., Garnero, E.J., Lay, T., Fouch, M.J., 2005. Azimuthal anisotropy in the D″ layer beneath the Caribbean. J. Geophys. Res. 110, B08301. doi:10.1029/2004JB003506.

McNamara, A.K., van Keken, P.E., Karato, S.-i., 2002. Development of anisotropic structure in the Earth's lower mantle by solid-state convection. Nature 416, 310–314.

Meade, C., Silver, P.G., Kaneshima, S., 1995. Laboratory and seismological observations of lower mantle isotropy. Geophys. Res. Lett. 22, 1293–1296.

Merkel, S., McNamara, A.K., Kubo, A., Speziale, S., Miyagi, L., Meng, Y., Duffy, T.S., Wenk, H.-R., 2007. Deformation of (Mg,Fe)SiO$_3$ post-perovskite and D″ anisotropy. Science 316, 1729–1732.

Moore, M.M., Garnero, E.J., Lay, T., Williams, Q., 2004. Shear wave splitting and waveform complexity for lowermost mantle structures with low-velocity lamellae and transverse isotropy. J. Geophys. Res. 103, B02319. doi:10.1029/2003JB002546.

Murakami, M., Hirose, K., Kawamura, K., Sata, N., Ohishi, Y., 2004. Post-perovskite phase transition in MgSiO$_3$. Science 304, 855–858.

Niu, F., Perez, A.M., 2004. Seismic anisotropy in the lower mantle: a comparison of waveform splitting of SKS and SKKS. Geophys. Res. Lett. 31, L24612. doi:10.1029/2004GL0211196.

Obrebski, M., Castro, R.R., Valenzuela, R.W., van Benthem, S., Rebollar, C.J., 2006. Shear-wave splitting observations at the regions of northern Baja California and southern Basin and Range in Mexico. Geophys. Res. Lett. 33, L05302. doi:10.1029/2005GL024720.

Oganov, A.R., Ono, S., 2004. Theoretical and experimental evidence for a post-perovskite phase of MgSiO$_3$ in Earth's D″ layer. Nature 430, 445–448.

Panning, M., Romanowicz, B., 2006. A three-dimensional radially anisotropic model of shear velocity in the whole mantle. Geophys. J. Int. 167, 361–379.

Plomerová, J., Achauer, U., Babuska, V., Vecsey, L., 2007. Upper mantle beneath the Eger Rift (Central Europe): plume or asthenosphere upwelling? Geophys. J. Int. 169, 675–682.

Polet, J., Kanamori, H., 2002. Anisotropy beneath California: shear wave splitting measurements using a dense broadband array. Geophys. J. Int. 149, 313–327.

Restivo, A., Helffrich, G., 2006. Core–mantle boundary structure investigated using SKS and SKKS polarization anomalies. Geophys. J. Int. 165, 288–302.

Rokosky, J.M., Lay, T., Garnero, E.J., 2006. Small-scale lateral variations in azimuthally anisotropic D″ structure beneath the Cocos Plate. Earth Planet. Sci. Lett. 248, 411–425.

Silver, P.G., Chan, W.W., 1991. Shear wave splitting and subcontinental mantle deformation. J. Geophys. Res. 96, 16,429–16,454.

Sidorin, I., Gurnis, M., Helmberger, D.V., 1999. Evidence for a ubiquitous seismic discontinuity at the base of the mantle. Science 286, 1326–1331.

Thomas, C., Wookey, J., Simpson, M., 2007. D″ anisotropy beneath Southeast Asia. Geophys. Res. Lett. 34, L04301. doi:10.1029/2006GL028965.

Trampert, J., Deschamps, F., Resovsky, J., Yuen, D.A., 2004. Probabilistic tomography maps chemical heterogeneities throughout the lower mantle. Science 306, 853–856.

Tsuchiya, T., Tsuchiya, J., Umemoto, K., Wentzcovitch, R.M., 2004. Phase transition in MgSiO$_3$ perovskite in the Earth's lower mantle. Earth Planet. Sci. Lett. 224, 241–248.

Vidale, J.E., 1986. Complex polarization analysis of particle motion. Bull. Seism. Soc. Am. 71, 1511–1530.

Wang, Y., Wen, L., 2007. Complex seismic anisotropy at the border of a very low velocity province at the base of the Earth's mantle. J. Geophys. Res. 112, B09305. doi:10.1029/2006JB004719.

Wen, L., Helmberger, D.V., 1998. Ultra-low velocity zones near the core–mantle boundary from broadband PKP precursors. Science 279, 1701–1703.

Wenk, H.R., Speziale, S., McNamara, A.K., Garnero, E.J., 2006. Modeling lower mantle anisotropy development in a subducting slab. Earth Planet. Sci. Lett. 245, 302–314.

Wentzcovich, R.M., Tsuchiya, T., Tsuchiya, J., 2006. MgSiO$_3$ postperovskite at D″ conditions. Proc. Natl. Acad. Sci. 103, 543–546.

Wookey, J., Kendall, J.M., 2007. Seismic anisotropy of post-perovskite and the lowermost mantle. In: Hirose, K., et al. (Ed.), Post-perovskite: the Last Mantle Phase Transition. Geophys. Monogr., vol. 174. AGU, Washington, DC, pp. 171–189.

Wookey, J., Kendall, J.-M., 2008. Constraints on lowermost mantle mineralogy and fabric beneath Siberia from seismic anisotropy. Earth Planet Sci. Lett. 275, 32–42.

Wookey, J., Kendall, J.-M., Rümpker, G., 2005a. Lowermost mantle anisotropy beneath the North Pacific from differential S-ScS splitting. Geophys. J. Int. 161, 829–838.

Wookey, J., Stackhouse, S., Kendall, J.-M., Brodholt, J., Price, G.D., 2005b. Efficacy of the post-perovskite phase as an explanation for lowermost-mantle seismic properties. Nature 438, 1004–1007.

Wüstefeld, A., Bokelmann, G., 2007. Null detection in shear-wave splitting measurements. Bull. Seism. Soc. Am., 97, 1204–1211.

Wüstefeld, A., Bokelmann, G., Barruol, G., Zaroli, C., 2007. Splitlab: a shear-wave splitting environment in Matlab. Comput. Geosci 34, 515–528.

Yamazaki, D., Karato, S.-i., 2002. Fabric development in (Mg,Fe)O during large strain, shear deformation: implications for seismic anisotropy in Earth's lower mantle. Phys. Earth Planet. Inter. 131, 251–267.

Yamazaki, D., Karato, S.-i., 2007. Lattice-preferred orientation of lower mantle materials and seismic anisotropy in the D″ layer. In: Hirose, K., et al. (Ed.), Post-perovskite: the Last Mantle Phase Transition. Geophys. Monogr., vol. 174. AGU, Washington, DC, pp. 69–78.

Yamazaki, D., Yoshino, T., Ohfuji, H., Ando, J.-i., Yoneda, A., 2006. Origin of seismic anisotropy in the D″ layer inferred from shear deformation experiments on post-perovskite phase. Earth Planet. Sci. Lett. 252, 372–378.

Yoshino, T., Yamazaki, D., 2007. Grain growth kinetics of CaIrO$_3$ perovskite and post-perovskite, with implications for rheology of D″ layer. Earth Planet. Sci. Lett. 255, 485–493.